Shear Behavior of RC Circular Members

円形断面を有するRC部材のせん断挙動

Hongxing QIU, Kazuo YAMADA, Yasuzi SAKOU
邱 洪興†, 山田和夫‡, 酒向靖二‡†

Abstract The theory of shear behavior for RC circular members proposed in this paper is based on the diagonal compression field theory. The aggregate interlock of cracked section and the dowel action of longitudinal steel are ignored in the model. The influence of non-uniform of stirrup strain is discussed and it is thought that the influence is negligible. According the model, the shear stress-shear strain relationship for circular members can be predicted. For ascending branch, predicted curves show a good agreement with test curves. For specimens with light stirrups, there is difference between theoretical curve and test curve in descending branch. The theory predicts that the angle of diagonal compression will vary with shear stress. Before the yield of stirrup, the inclined angle will increase as stress increase; and will decrease after the stirrup have yielded. While concrete strain has reached peak strain, the inclined angle will increase once again. The shear strength equation proposed in this paper which includes the effect of axial force is expressed in a simple form which is convenient to use, and is consistent with one which does not include axial force.

Keyword shear stress; shear strength; axial forces; cracks; reinforced concrete; stirrups

1. Introduction

The shear behavior of RC members is one of which researchers are very interested in. Although comprehensive research[1),2)] on this field has been made by many students, to date very little work has been reported on the shear behavior of RC circular members. The circular members are used as piles and column of building and traffic engineering more and more extensive. In this paper the diagonal compression field theory is applied to predict shear behavior of RC circular members. The diagonal compression field theory is proposed by Wagner[3)] in 1929 to study the post-bucking shear resistance of thin webbed metal beams. Mitchell and Collins[4),5)] had developed the models for structural concrete in pure torsion and shear by this theory. They assumed that after cracking the concrete can resist no tension and concrete in web is replaced by a idealized diagonal compression field.

Fig.1 is a photograph of the test section of a reinforced concrete circular member tested in shear at Aichi Institute of Technology. The mag-

† 中国東南大学土木工学科 (中国南京)
‡ 愛知工業大学工学部建築学科 (豊田市)
‡†愛知工業大学大学院建設システム工学専攻

nitudes of the applied loads for this member were arranged so that the moment was zero at the midpoint of the test region.

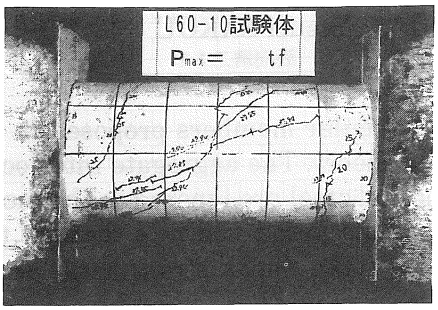

Fig. 1 Circular section specimen

We will only consider the section where the effects of flexural moment and disturbances of point loads are negligible. However, the effects of axial load will be discussed finally.

Due to the cracks considerable variations will arise in the local strains(hence stresses) of a member. Rather than trying to deal with variable local strains and stresses, we will consider only the average strains and stresses.

2. Equilibrium Conditions

Consider the equilibrium requirement in vertical direction for the free body shown in Fig.2.

If we ignore the dowel force of the longitudinal steel, all of the shear force at the section must be carry by concrete, that is

$$Q = P_c \sin\alpha \qquad (1)$$

where Q=shear force; α=angle of diagonal compression to longitudinal axis of member; $P_c = \pi R_m^2 \cos\alpha\sigma_c$ is resultant force of diagonal compression in concrete; R_m=effective radius of circular section, is taken from internal side of stirrups; σ_c=average concrete stress in diagonal compression direction.

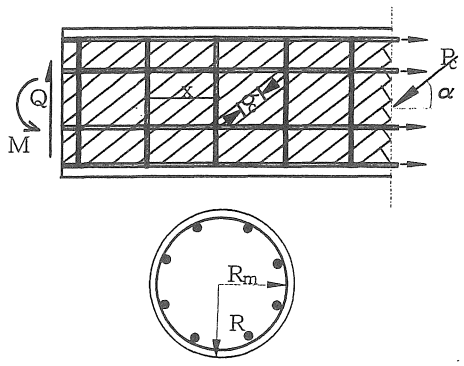

Fig. 2 Forces in free body

Defining $\tau = Q/\pi R_m^2$ as nominal shear stress. Thus, Eq.(1) becomes

$$\sigma_c = \frac{\tau}{\sin\alpha\cos\alpha} \qquad (1\text{-a})$$

Consider the equilibrium condition in vertical direction for the inclined section shown in Fig.3. Similarly, we ignore the dowel force of the longitudinal steel. Further, if the aggregate interlock of cracked section is ignored, all of the shear force at the section must be carry by stirrups. Because the direction of force in different location is variable, the integral is needed. The stirrups are equivalent to uniform stresses, $a_w\sigma_s / x$ (a_w=area of stirrup; x=spacing of stirrups; σ_s=stress of stirrups). Thus

$$Q = 2\int_{-\pi/2}^{\pi/2} \frac{a_w\sigma_s}{x} dz\cos\theta \qquad (2)$$

It is noted that the equation for

intersecting line of cylinder and inclined plane, $z = R_m \cot\alpha \sin\theta$. Substituting $dz = R_m \cot\alpha \cos\theta d\theta$ into Eq.(2), by integral, one obtains

$$\sigma_s = \frac{2\tau \sin\alpha}{p_w \cos\alpha} \qquad (2\text{-a})$$

where $p_w = 2a_w / xR_m$ is stirrup ratio.

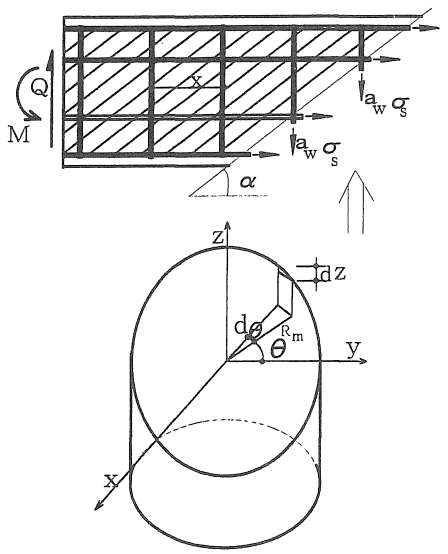

Fig. 3 Forces in inclined section

3. Average Stress-Average Stain Relationships

For the steel it will be assumed that the relationship between the local stain at a particular location, ε, and the local stress at this same location, σ, is given by $\sigma = E_s\varepsilon \le f_y$. As some of the steel strain are below the yield strain(ε_y) while some are above(the steel strain is often not uniform), the relationship between the average strain and the average stress will not be given precisely by this equation.

Assume steel strain in some a region, h, is linear distribution. This assumption is shown in Fig.4.

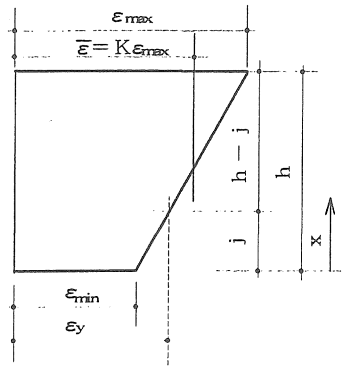

Fig.4 Distribution of stirrup stress

Defining the ratio of average strain to maximum strain in this region as non-uniform factor K, that is $K = \bar{\varepsilon} / \varepsilon_{max}$, thus, in region j, $j = \frac{h}{2}[\frac{K}{1-K}\frac{\varepsilon_y}{\bar{\varepsilon}} - \frac{2K-1}{1-K}]$, the steel strain is below the yield strain ε_y, and the steel strain in any location $\varepsilon_x = \frac{2(1-K)x}{hK}\bar{\varepsilon} + \frac{2K-1}{K}\bar{\varepsilon}$. By the following integral, the relationship between the average strain and the average stress can be obtained.

$$\bar{\sigma} = \frac{1}{h}[\int_0^j \varepsilon_x E_s dx + \int_j^h \varepsilon_y E_s dx]$$

$$\bar{\sigma} = [\frac{1}{2(1-K)}(\frac{\varepsilon_y}{\bar{\varepsilon}}) - \frac{K}{4(1-K)}(\frac{\varepsilon_y}{\bar{\varepsilon}})^2 - \frac{(2K-1)^2}{4K(1-K)}]\bar{\varepsilon}E_s \qquad (3)$$

The using region for Eq.(3) are $\varepsilon_{max} \ge \varepsilon_y$ and $\varepsilon_{min} \le \varepsilon_y$, i.e. $K\varepsilon_y \le \bar{\varepsilon} \le \frac{K}{2K-1}\varepsilon_y$. Thus, the relationship between the average strain and the average stress can be expressed by

$$\begin{cases} \sigma_s = \varepsilon_s E_s & (\varepsilon_s < K\varepsilon_y) \\ \sigma_s = [\frac{1}{2(1-K)}(\frac{\varepsilon_y}{\varepsilon_s}) - \frac{K}{4(1-K)}(\frac{\varepsilon_y}{\varepsilon_s})^2 \\ \quad -\frac{(2K-1)^2}{4K(1-K)}]\varepsilon_s E_s & (K\varepsilon_y \le \varepsilon_s \le \frac{K}{2K-1}\varepsilon_y) \\ \sigma_s = \varepsilon_y E_s & (\varepsilon_s > \frac{K}{2K-1}\varepsilon_y) \end{cases} \quad (3\text{-a})$$

where Es = Young's modulus of stirrup.

For convenience, the average strain and average stress are labeled ε_s, σ_s, respectively. This relationship is shown in Fig. 5.

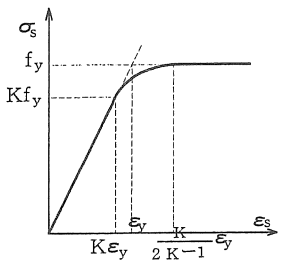

Fig. 5 Stress-strain relationship of stirrup

The stress-strain relationship of concrete in the direction of diagonal compression is represented by the following equations.

$$\sigma_c = \lambda f_c [2\frac{\varepsilon_c}{\varepsilon_0} - (\frac{\varepsilon_c}{\varepsilon_0})^2] \quad (4)$$

Where f_c = cylinder compression strength of concrete; ε_c = average compression strain of concrete in diagonal compression direction; ε_0 = concrete compression strain corresponding to peak stress; λ = effective index of concrete strength.

Taking value of ε_0 should accord with stress—strain curve.

$$E_c = \frac{d\sigma_c}{d\varepsilon_c}|_{\varepsilon_c=0} \Rightarrow \varepsilon_0 = \frac{2\lambda f_c}{E_c}$$

The effective index of concrete take care of the softening phenomenon of concrete in biaxial stresses. Based on the analysis of 153 shear tests of simple T-beam, Nielsen and Brasestrup[6] found this factor was equal to 0.72. It is thought in references[7] that this factor relates relative shear stiffness of sections. The relative shear stiffness of sections will increase as longitudinal reinforcement ratio rise and decrease as the ratio of shear span to depth rise. Based on regression analysis of 178 shear tests of reinforced concrete T-beams (I-beams), the following empirical equation is proposed in references[7].

$$\lambda = 0.6 + \frac{0.15}{M/Q \cdot d} + \frac{\beta_t - 0.5}{10} \quad (5)$$
$$(0.5 \le M/Q \cdot d \le 3, \quad 0.5 \le \beta_t \le 2)$$

where $\beta_t = p_t f_{ty} / f_c$, is longitudinal steel index.

4. Compatibility Condition

The relationship between concrete strain, stirrup strain and shear strain of section can be founded by virtual work method. Acting a pair of unit virtual force on member shown in Fig.6.

It is noted that there are virtual stresses only in dy region. The virtual stresses σ_c, σ_s can be expressed by use of Eq.(1-a) and Eq.(2-a), respectively.

$$\begin{cases} \sigma_c = \dfrac{1}{\pi R_m^2 \sin\alpha \cos\alpha} \\ \sigma_s = \dfrac{2\tan\alpha}{\pi R_m^2 p_w} \end{cases} \quad (6)$$

Assume longitudinal steel is rigid, i.e. the strain of longitudinal steel is ignored. It is noted that the stresses and strains of concrete and stirrup are not related to location of sections. By virtual work equation, one obtains

$$\gamma dy \times 1 = \int_V \vec{\sigma} \cdot \vec{\varepsilon}$$

$$= \int_0^{dy} \sigma_c \varepsilon_c \pi R_m^2 dx + (\sigma_s \varepsilon_s) \times (2\pi R_m a_m) \times (\frac{dy}{x})$$

$$\gamma = \frac{\varepsilon_c}{\sin\alpha \cos\alpha} + \frac{2\varepsilon_s \sin\alpha}{\cos\alpha} \quad (7)$$

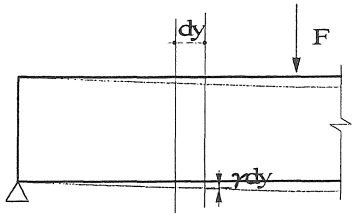

a) Actual displacement and strain

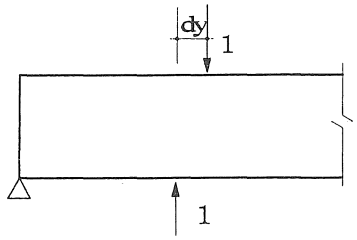

b) Virtual force and stress

Fig. 6 Acting a pair of unit virtual force on member

The inclined angle of diagonal compression would adjust itself so that the strain energy in the system would be minimized[3]. The internal energy will be minimum if the external work done, and hence for a given load, the external displacement(i.e. shear stain) is a minimum. This means $\frac{d\gamma}{d\alpha} = 0$, and leads to

$$\sin^2\alpha = \frac{\varepsilon_c}{2(\varepsilon_c + \varepsilon_s)} \quad (8)$$

Eq. (8) is the compatibility condition of concrete strain and stirrup strain.

5. Prediction of Shear Behavior

The expression of ultimate shear strength is related to the balanced stirrup index that the stirrup starts to yield and concrete reaches its ultimate capacity at precisely the same load. By substituting $\varepsilon_c = \varepsilon_0, \varepsilon_s = \varepsilon_y$ into Eq. (8), one obtains the inclined angle of diagonal compression of balanced section in ultimate state

$$Sin^2\alpha_b = \frac{1}{2(1+\zeta_b)} \quad (8\text{-a})$$

where $\zeta_b = \varepsilon_y / \varepsilon_0$.

By substituting the value of α obtained from Eq. (8-a) and $\sigma_c = \lambda f_c, \sigma_s = f_{wy}$ into Eq. (1-a) and Eq.(2-a) respectively, one obtains the following equation for balanced stirrup index:

$$\beta_{w,b} = \frac{\lambda}{1+\zeta_b} \quad (9)$$

where $\beta_{w,b}$= balanced stirrup index.

If stirrup index $\beta_w < \beta_{w,b}$, stirrups will yield before the beam reaches its ultimate state. By substituting $\sigma_c = \lambda f_c, \sigma_s = f_{wy}$, into Eq. (1-a) and Eq.(2-a) respectively, the inclined angle of diagonal compression in ultimate state is given by the expression

$$Sin\alpha = \sqrt{\frac{\beta_w}{2\lambda}} \quad (8\text{-b})$$

By substituting the value of α obtained from Eq. (8-b) into Eq. (1-a)

and substituting $\varepsilon_c = \varepsilon_0$, the ultimate strength can be obtained

$$\tau_u / f_c = \sqrt{\frac{\beta_w}{2}(\lambda - \frac{\beta_w}{2})} \qquad (10)$$

If stirrup index $\beta_w > \beta_{w,b}$, stirrup will not yield in ultimate state. It is approximately thought the ultimate shear strength of over-reinforced section is equal to the ultimate shear strength of the balanced section, that is, taking $\beta_w = \beta_{w,b}$ in Eq. (10).

Comparing Eq. (10) with ultimate shear strength for T-beams[7], it is found that the $\beta_w/2$ for circular members is correspond to β_w for T-beams.

The equilibrium conditions, the compatibility condition, and the stress-strain relationships have been obtained, so we are now able to make a prediction of circular member loaded in shear.

By substituting Eq. (3-a), Eq. (4) into Eq. (2-a), Eq. (1-a), respectively, one obtains

$$\frac{\tau}{f_c} = \lambda[2\frac{\varepsilon_c}{\varepsilon_0} - (\frac{\varepsilon_c}{\varepsilon_0})^2]\sin\alpha\cos\alpha \qquad (11)$$

$$\begin{cases} \dfrac{\tau}{f_c} = \dfrac{\beta_w \cos\alpha\varepsilon_s}{2\varepsilon_y \sin\alpha} & (\varepsilon_s < K\varepsilon_y) \\ \dfrac{\tau}{f_c} = \dfrac{\beta_w \cos\alpha\varepsilon_s}{2\varepsilon_y \sin\alpha}[\dfrac{1}{2(1-K)}(\dfrac{\varepsilon_y}{\varepsilon_s}) - \dfrac{K}{4(1-K)}(\dfrac{\varepsilon_y}{\varepsilon_s})^2 & \\ \quad - \dfrac{(2K-1)^2}{4K(1-K)}] & (K\varepsilon_y \le \varepsilon_s \le \dfrac{K}{2K-1}\varepsilon_y) \\ \dfrac{\tau}{f_c} = \dfrac{\beta_w \cos\alpha}{2\sin\alpha} & (\varepsilon_s > \dfrac{K}{2K-1}\varepsilon_y) \end{cases} \qquad (12)$$

where $\beta_w = f_{wy}p_w / f_c$ is stirrup index.

The shear strain of sections in a certain magnitude of shear can be prediction by above model. Eq. (7), (8), (11) and (12) include five unknowns, ε_s, ε_c, γ, τ and α. When shear stress τ is given, the other four can be solved. So shear strain can be obtained as follows.

a) Select a value for τ;
b) Assume a value of α;
c) Calculate ε_c by using Eq. (11);
d) Calculate ε_s by using Eq. (12);
e) Calculate α by using Eq. (8);
f) If the angle calculated does not agree with the estimated angle, then a new estimate of α could be made and repeat the step c) to step e).
g) Calculate γ by using Eq. (7).

To apply the theory, it is necessary to know the factor λ. Because the shear tests of RC circular members are not enough to make regression analysis, here Eq. (5) is used.

The prediction of shear behavior for specimen L60-05 (whose section parameters are given in Table 1) is shown in Fig. 7. It provides four

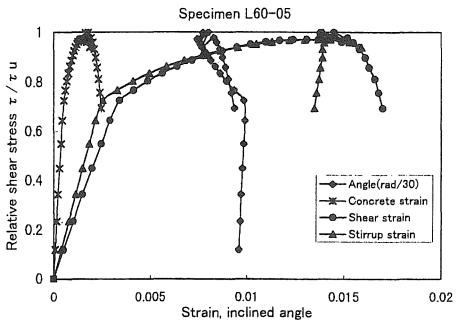

Fig. 7 Shear behavior for specimen L60-05

curves: shear stress-shear strain relationship, shear stress-concrete strain relationship, shear stress-stirrup strain relationship and shear stress-inclined angle relationship. The terminal point of curves correspond a concrete strain of 0.0033λ. The longi-

tudinal coordinate is expressed in dimensionless parameter τ/τ_u.

Prior to stirrup yield, the relationships between shear stress and shear strain are approximately linear. After the stirrups have yielded, there is a marked drop in the stiff of specimen. As shear stress has reached its peak stress, there is a undulate in curves. The same phenomenon is found in tests. As ultimate load is reached, the needle of test machine rocks. It is thought that the peak is unstable.

It can be seen from Fig.7 that the angle of diagonal compression varies with shear stress. The angle of diagonal compression will depend on the ratio of stirrup strain to concrete strain(see Eq. (8)). Before the yield of stirrups, because of nonlinear of concrete, the increase in concrete strain is greater than stirrup, so the inclined angle will increase as shear stress increase. After the stirrups have yielded, the stirrup stress will remain at a constant value. From Eq. (2-a), it can be known that in order to increase the applied shear the angle of diagonal compression must decrease.

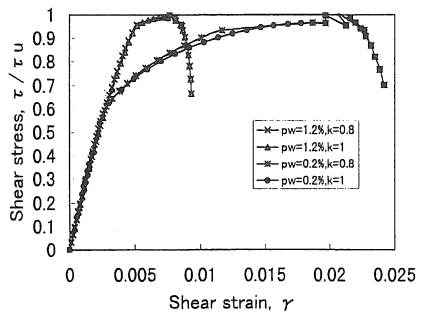

Fig. 8 Influence of non-uniform of stirrups

Fig. 8 shows the theoretical curve of members which have different stirrup ratio and non-uniform coefficient. It can be seen that influence of non-uniform of stirrups on shear behavior is inconsiderable. Above Fig. 7 does not consider the non-uniform of stirrups.

6. The Effect of Axial Force on Shear Strength

Fig. 9 shows that if there is a compression stress σ_c in diagonal direction, it is necessary to have compression stress and shear stress on vertical plane, i.e. longitudinal direction. For Mohr's stress circle, the magnitude of longitudinal compression stress, σ_l, is

$$\sigma_l = \frac{\tau}{\tan\alpha} \tag{13}$$

Eq. (13) can be expressed as

$$\tau = \sigma_l \tan\alpha \tag{13-a}$$

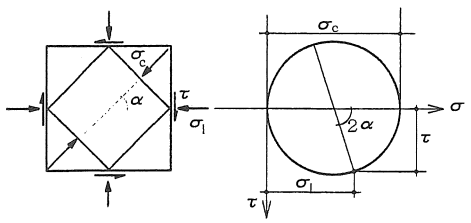

Fig. 9 Unite element and Mohr's circle

While axial compression force N is acted on the member, stress σ_l will increase, and results in the variation of shear stress. For simplicity, It is assumed that while axial force is acted, the angle of diagonal compression will not vary. Taking differentiation to Eq. (11-a), one obtains

$$\Delta\tau = \tan\alpha \Delta\sigma_l \qquad (13\text{-b})$$

It is noted that because of axial force, the increase in longitudinal compression stress is $\Delta\sigma_l = N/(\pi R^2 + na_t)$, thus

$$\Delta\tau = \tan\alpha \frac{N}{(\pi R^2 + na_t)} \qquad (13\text{-c})$$

Substituting Eq. (8-b) into Eq. (13-c) and using Eq. (10), the ultimate shear strength which includes the effect of axial force is given

$$\frac{\tau_u}{f_c} = \sqrt{\frac{\beta_w}{2}(\lambda - \frac{\beta_w}{2})} + \frac{2\sqrt{\frac{\beta_w}{2}(\lambda - \frac{\beta_w}{2})}}{2\lambda - \beta_w}\frac{\sigma_N}{f_c}$$

Because β_w is much smaller than 2λ, above equation can be approximately expressed as

$$\frac{\tau_u}{f_c} \approx (1 + \frac{\sigma_N}{\lambda f_c})\sqrt{\frac{\beta_w}{2}(\lambda - \frac{\beta_w}{2})} \qquad (14)$$

where $\sigma_N = \frac{N}{\pi R^2 + na_t}$; a_t=area of longitudinal steel; n=the ratio of Young's modulus of steel to concrete. While $\sigma_N = 0$, Eq. (14) is same as Eq. (10).

7. Comparison with Tests

Eight circular specimens are tested. Except two specimens without stirrup, a total of 6 test specimens which are used to compare with the proposed theory are listed in Table 1. The two specimens of them are acted axial compression force.

Fig. 10 and Fig. 11 show the relationships between shear stress and shear strain for specimen L60-05 and specimen L90-10, respectively. A test shear strain is calculated by dividing the measured relative shear dis-placement by the gage distance. In this test, the gage distances are 600mm and 900mm, respectively.

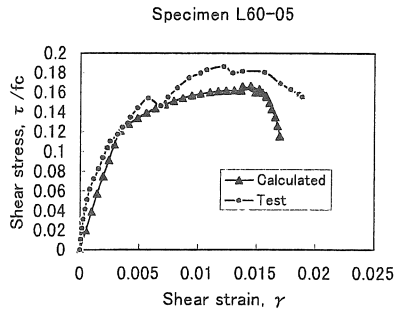

Fig.10 Shear stress-shear strain curves for specimen L60-05

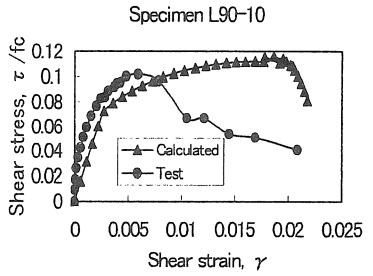

Fig. 11 Shear stress-shear strain curves for specimen L90-10

From Fig. 10 and Fig. 11, it can be seen that the predicted shear behavior for ascending branch shows a good agreement with test. It should be mentioned that the diagonal compression field theory is not intended for the prediction of behavior before cracking. Tests in Fig. 10 and Fig. 11 show that the specimens before cracking are stiffer than those predicted. Contrarily, after cracking the stiff of theoretical curve is greater than test curve's one. This can be expl-

Table 1 Comparison of theoretical and experimental results for shear strength

No.	Specimen	Diameter (mm)	M/QD	σ_N (MPa)	f_c (MPa)	p_t (%)	f_{ty} (MPa)	p_w (%)	f_{wy} (MPa)	$(\tau_u / f_c)^t$	$(\tau_u / f_c)^c$	τ_u^c / τ_u^t
1	L60-10	300	1.0	0	26.85	4.92	426	0.2	493	0.091	0.115	1.121
2	L60-05	300	1.0	0	26.85	4.92	426	0.4	493	0.186	0.162	0.871
3	L60-05F	300	1.0	5.467	26.85	4.92	426	0.4	493	0.173	0.206	1.191
4	L90-10	300	1.5	0	26.85	4.92	426	0.2	493	0.102	0.112	1.098
5	L90-05	300	1.5	0	26.85	4.92	426	0.4	493	0.120	0.156	1.30
6	L90-05F	300	1.5	5.467	26.85	4.92	426	0.4	493	0.166	0.201	1.213

Note: Superscript t denotes test results; superscript c denotes calculated values.

ained by the fact that the strain of longitudinal steel is ignored in the model.

There is difference between theoretical curve and test curve in descending branch, especially for specimen L90-10. The descending branch of RC members is probably subject to influence of test conditions and the peak is unstable. This phenomenon is much clear for the specimens with light steel.

Table 1 shows that the calculated shear strengths are mostly greater than the test values. The mean value of the ratio of the calculated shear strength to measured shear strength is 1.132 and the deviation coefficient is 0.129. A probable cause is that the Eq. (5) which is based on regression analysis of shear tests of T-beams and I-beams, and is used for determining factor λ does not very suit to circular members.

8. Discussion and Conclusions

This paper has first used the diagonal compression field theory for the behavior of reinforced concrete circular members monotonically loaded in shear. By proposed model, the shear stress-shear strain relationship for circular members can be predicted. For ascending branch, predicted curves show a good agreement with test curves. For descending branch, there is difference between theoretical curve and test curve, especially for specimen which is lightly reinforced in stirrup. It thought that the descending branch of RC members is subject to influence of test conditions. On the other hand, the diagonal compression field theory has showed better accuracy for specimens with heavy stirrups than the specimens with light stirrups. All six specimens in this test have light stirrups.

According to the theory, it is showed that the influence of non-uniform of stirrup stress on shear behavior is inconsiderable. The general elastic-plastic stress-strain curve for steel can be used as the relationship between the average stress and average strain for stirrup.

The equation for shear strength of circular members is similar to the one of T-beams. The ultimate shear strength of circular members with stirrup index β_w is correspond to the ultimate shear strength of T-beams with stirrup index $\beta_w/2$. The shear strength equation proposed in this paper which includes the effect of axial force is consistent with one which does not include axial force. While axial force is equal to zero, both are same.

The calculated shear strength are

mostly greater than the test values. The factor λ for circular members is probably different to one for T-beams. The paper contains only six test specimens to compare with theory. More tests of circular specimens are required for determining factor λ.

References

1. ACI-ASCE Committee 426, "The Shear Strength of Reinforced Concrete Members," *Journal of the Structural Division*, ASCE, Vol.99, ST6, June, pp.1091～1187, 1973.

2. ASCE-ACI Committee 445, "Recent Approaches to Shear Design of Structural Concrete," *Journal of Structural Engineering*, Vol. 124, No. 12, pp. 1375 ～1417, December 1998.

3. Wagner, H., "Ebene Blechwandtrager mit sehr dunnem Stegblech," *Zeitschrift fur Flugtechnik und Motorluftschiffahrt* Berlin, Germany, Vol.20, Nos. 8-12, 1929.

4. Mitchell, D., and Collins, M. P., "Diagonal Compression Field Theory--A Rational Model for Structural Concrete in Pure Torsion," *American Concrete Institute Journal*, vol.71, pp. 396～408, Aug., 1974.

5. Collins, Michael P., "Towards a Rational Theory for RC members in Shear," *Journal of the Structural Division, ASCE,* Vol. 104, No. 4, pp649～666, April, 1978.

6. Nielsen, M. P., and Braestrup, M. W., "Plastic Shear Strength of Reinforced Concrete Beams," *Bygningsstatiske Meddeleser,* Copenhagen, Denmark, Vol.46, No3, pp. 61～99, 1975.

7. 邱洪兴，丁大均和蒋永生，"钢筋轻竹料砼T形截面梁剪切强度的试验研究，" *东南大学学报*，南京，中国，Vol.23, No.4, pp. 93～99, July, 1993.

8. 酒向靖二，山田和夫，山本俊彦，浅井陽一，"場所打ち鉄筋コンクリート杭の実験（その1:せん断実験）"，*日本建築学会東海支部研究報告集*，第37号，pp. 289～292, 1999.

9. 崔　益暢，二羽淳一郎，"格子モデルによるRCはりのせん断性状の解析的評価，" *コンクリート工学年次論文報告集*，Vol. 16, No. 2, pp. 563～568 , 1994.

10. 二羽淳一郎，崔　益暢，田辺忠顕，"鉄筋コンクリートはりのせん断耐荷機構に関する解析的研究"，" *土木学会論文集*，No 508/V-26, pp. 79～88, 1995.

(受理　平成11年3月20日)